Bioorganic Chemistry 56 (2014) 67–74

Contents lists available at ScienceDirect

Bioorganic Chemistry

journal homepage: www.elsevier.com/locate/bioorg

The interaction of a cobalt porphyrin with cancer-associated nitrosamines

Feiyan Tao [a,b], Ya Dai [b,*], Changguo Wang [b], Guanglin Feng [b], Dongliang Li [b], Kuoyan Ma [b], Lijun Zhu [b], Lanlan Tan [b], Xiaoqi Yu [a,*]

[a] Key Laboratory of Green Chemistry and Technology, Ministry of Education, College of Chemistry, Sichuan University, Chengdu 610064, China
[b] Harmful Components and Tar Reduction in Cigarette, Sichuan Key Laboratory Technical Research Center, Chuanyu Branch of China Tobacco Corporation, Chengdu 610066, China

ARTICLE INFO

Article history:
Received 27 February 2014
Available online 31 July 2014

Keywords:
Metalloporphyrin
Cobalt porphyrin
TSNAs
Coordination interaction
Hemin
Association constants

ABSTRACT

A cobalt porphyrin (**CY-B**) was presented, and its interaction with tobacco-specific nitrosamines **(TSNAs)** was investigated by UV–Vis spectroscopy and high-resolution mass spectrometry. The results revealed that the stoichiometry of the host–guest interaction was 1:2 and that the binding constant between **CY-B** and **TSNAs** was within the range of 0.78×10^8–7.83×10^8 M^{-2}. The coordination strength between **CY-B** and **TSNAs** decreased in the sequence of NNN > NAB > NAT > NNK based on the binding constant. The interaction mechanism of **CY-B** with **TSNAs** involved a coordination interaction, and the π–π interaction between the porphyrin macrocycle and the aromatic frame of the **TSNAs** pyridines may also have been a driving force. The measured thermodynamic properties demonstrated that the reaction of **CY-B** with **TSNAs** was spontaneous and that the driving force for the interaction was a change in enthalpy. The reaction was exothermic, and an increasing temperature inhibited the interaction. The IR spectrum of the complex revealed that the —N—N=O group of **TSNAs** and the metal cobalt of **CY-B** formed the six-coordinate complex.

1. Introduction

Nitrosamines (R_2N—N=O; R = alkyl, aryl) belong to the class of *N*-nitroso compounds, which are present in a wide range of environments including cigarette smoke, beer, saliva, and the rubber nipples used for feeding bottles [1,2]. *N*-nitrosamines are ubiquitous yet toxic compounds and potent carcinogens, primarily because of their ability to alkylate DNA [3]. They require metabolic activation by the heme-containing enzyme cytochrome P450 in the liver, lung, or nasal tissues to exert their carcinogenic effects [4]. The interaction of nitrosamines with the active site of cytochrome P450 can occur *via* two main paths [5] (Fig. 1). The Type I interaction is typical of cytochrome P450 monooxygenase systems, in which the nitrosamine binds to the protein pocket site near the iron center in preparation for its α-hydroxylation and subsequent chemical modification to generate highly reactive organic species. The Type II interaction places the nitrosamine in direct contact with the iron center in cytochrome P450. Despite this important observation by Appel and co-workers, very little is known about the Type II hemenitrosamine interaction, except that Guengerich and coworkers have reported the coordination interaction of ferric tetraphenylporphyrin with nitroamine [6]. Therefore, it is important and necessary to build a new model to investigate the interaction of these compounds.

Tobacco-specific nitrosamines (TSNAs) are known components of tobacco products and tobacco smoke [7]. *N*-nitrosonornicotine (NNN), 4-(methylnitrosamino)-1-(3-pyridyl)-1-butanone (NNK), *N*-nitrosoanata-bine (NAT), and *N*-nitrosoanabasine (NAB) are the most common TSNAs (Fig. 2) and play an important role in tobacco-induced carcinogenesis [8]. Among these compounds, the primary metabolites of NNK (4-(methylnitrosamino)-1-(3-pyridyl)-1-butanol; NNAL) and *N*-nitrosonornicotine (NNN) are the most carcinogenic. In fact, NNK and NNAL are procarcinogens that require metabolic activation by cytochrome P450 enzymes to express their biological activity. α-Hydroxylation of the methylene carbon atoms adjacent to the *N*-nitroso group is believed to result in the metabolic activation of NNK and NNAL because the unstable intermediates that are produced decompose to alkyldiazohydrox-

Abbreviations: TSNAs, tobacco-specific nitrosamines; NNN, *N*-nitrosonornicotine; NNK, 4-(methylnitrosamino)-1-(3-pyridyl)-1-butanone; NAT, *N*-nitrosoanatabine; NAB, *N*-nitrosoanabasine; B–H equation, Benesi–Hildebrand equation; HR-MS, high resolution mass spectrometry.

* Corresponding authors.
E-mail addresses: dycy@263.net (Y. Dai), xqyu@scu.edu.cn (X. Yu).

http://dx.doi.org/10.1016/j.bioorg.2014.07.007
0045-2068/

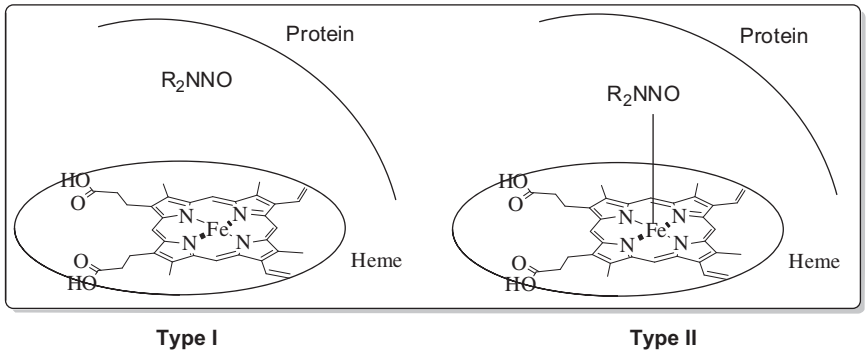

Fig. 1. Type I and Type II interactions of nitrosamines with the active site of cytochrome P450.

ide, which can alkylate DNA and other cellular macromolecules [9]. Although metabolism *via* the α-hydroxylation of the methylene carbon atoms adjacent to the *N*-nitroso group and the resulting gene mutation are understood, very little is known about nitrosamine (especially TSNA) metabolic activation by cytochrome P450 enzymes that express their biological activity *via* Type II interactions. To the best of our knowledge, no study has examined the interactions of metalloporphyrins with **TSNAs**.

In addition, hemoglobin-containing ferric porphyrins and other porphyrins have been shown to be promising as cigarette filter additives for removing hazardous smoke components, such as carcinogenic *N*-nitro compounds [10–12]. However, the detailed mechanism for this interaction remains poorly understood. In this study, we present a cobalt porphyrin compound (**CY-B**) whose interactions with **TSNAs** were studied in detail by UV–Vis spectroscopy and high-resolution mass spectrometry.

2. Experiments

2.1. General

^{1}H NMR spectra were measured on a Bruker AMX-400. The ^{1}H NMR (400 MHz) chemical shifts were given in ppm relative to internals reference TMS. ESI-MS and HR-MS spectral data were recorded on a Finnigan LCQ^{DECA} and a Bruker Daltonics BioTOF mass spectrometer, respectively. UV–Vis absorption spectra were recorded on a Hitachi PharmaSpec UV-1900 UV–Vis spectrophotometer. Unless otherwise noted, materials were obtained from commercial suppliers and were used without further purification.

Standardized NNK, NNN, NAT, NAB were obtained from Sigma–Aldrich (St. Louis, MO). Hemin was extracted from animal fresh blood in our laboratory [13]. All of the solvents were dried according to the standard methods prior to use. The solvents were either HPLC or spectroscopic grade in the optical spectroscopic studies. TLC analyses were performed on silica gel GF254. Reactions were monitored by TLC detection being carried out by UV or by iodine vapor.

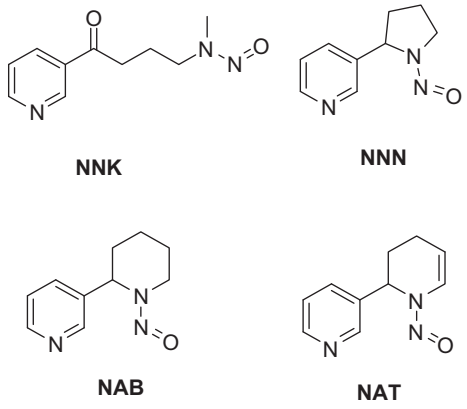

Fig. 2. Chemical structure of TSNAs.

2.2. Synthesis of metalloporphyrin ***CY-B***

2.2.1. Synthesis of ***CY-A***

To the bottom flask was added hemin (10.0 g, 15.34 mmol) and 100 mL of 33% HBr in HOAc, and the mixture was stirred at room temperature for 48 h. The resulting bromo-substituted protoporphyrin solution was used directly in the next step.

To the above solution, methanol (500 mL) was added slowly and the solution was refluxed for 8 h. Then the solvent was removed in vacuo, and the residue was suspended in water and adjusted pH to 8–9 with 2 M NaOH aq. solution. The solid was collected by filtration to give crude **CY-A**. The crude product was recrystallized from the mixture solvent of ethyl acetate and petroleum ether to afford **CY-A** [12] (7.6 g, 11.61 mmol) with 75.7% yield.

^{1}H NMR ($CDCl_3$): δ, ppm −3.66 (s, 2H, pyrrole-H), 2.28 (d, 6H, J = 4.4 Hz, $CH\underline{CH_3}$), 3.31 (m, 4H, $\underline{CH_2}COO$), 3.64–3.37 (m, 24H, OCH_3, CH_3), 4.43 (m, 4H, $\underline{CH_2}CH_2COO$), 6.07 (m, 2H, $CH_3\underline{CH}$), 10.10, 10.14, 10.53, 10.57 (4s, 4H, meso-H). ESI MS (positive ion mode) (rel. int.) m/z: 655 ($[M+H]^+$, 100). HRMS (ESI): m/z: 655.3469 ($[M+H]^+$, 100); calcd. for $C_{38}H_{46}N_4O_6$+H: 655.3417 ($[M+H]^+$, 100). UV–Vis (CH_2Cl_2): λ_{max}, nm ($\log\varepsilon$) = 399 (5.27), 498 (4.15), 532 (3.95), 569 (3.77) and 621 (4.62). IR: ν, cm^{-1} 3313.0, 1971.0, 2925.0, 2860.4, 1741.7, 1455.6, 1362.5, 1168.1, 1112.5, 1085.1, 964.9, 826.1, 743.0 and 678.5.

2.2.2. Synthesis of ***CY-B***

To 250 mg **CY-A** refluxing in 10 mL chloroform was added 1.0 mL of a boiling saturated solution of cobalt acetate in glacial acetic acid. After a few minutes' refluxing (about 5 min), the mixture was cooled and more chloroform was added and the chloroform solution was washed with water until free inorganic materials and of acetic acid. The solvent was dried over anhydrous Na_2SO_4, then concentrated to get the residue which was purified by column chromatography (Al_2O_3) to afford the **CY-B** [14] (185 mg) with 68.0% yield.

ESI MS (positive ion mode) (rel. int.) m/z: 711 ($[M]^+$, 100). HRMS (ESI): m/z: 711.2571 ($[M]^+$, 100); calcd. for $C_{38}H_{44}CoN_4O_6$: 711.2593 ($[M]^+$, 100). UV–Vis (CH_2Cl_2): λ_{max}, nm ($\log\varepsilon$) = 393 (5.47), 517 (4.22) and 551 (4.48). IR: ν, cm^{-1} 3442.3, 2927.2, 2866.2, 1730.9, 1434.4, 1355.6, 1251.2, 1163.6, 1093.7 and 831.8.5.

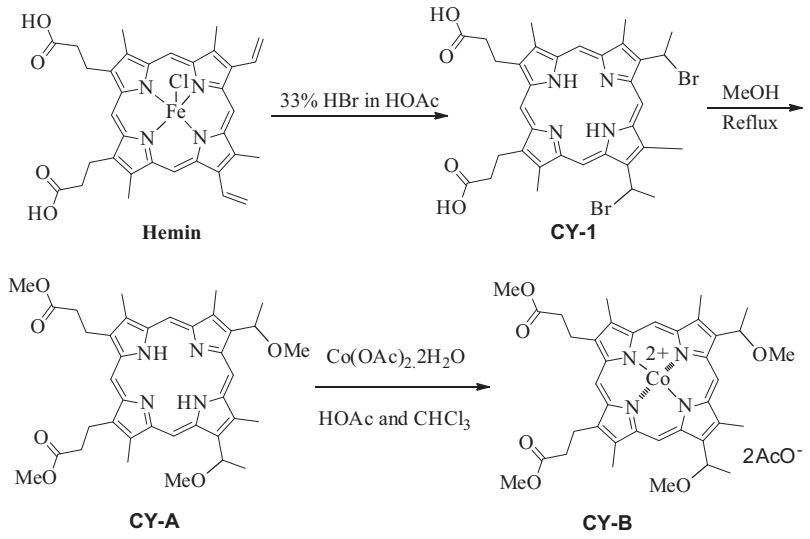

Scheme 1. Synthetic route for metalloporphyrin **CY-B**.

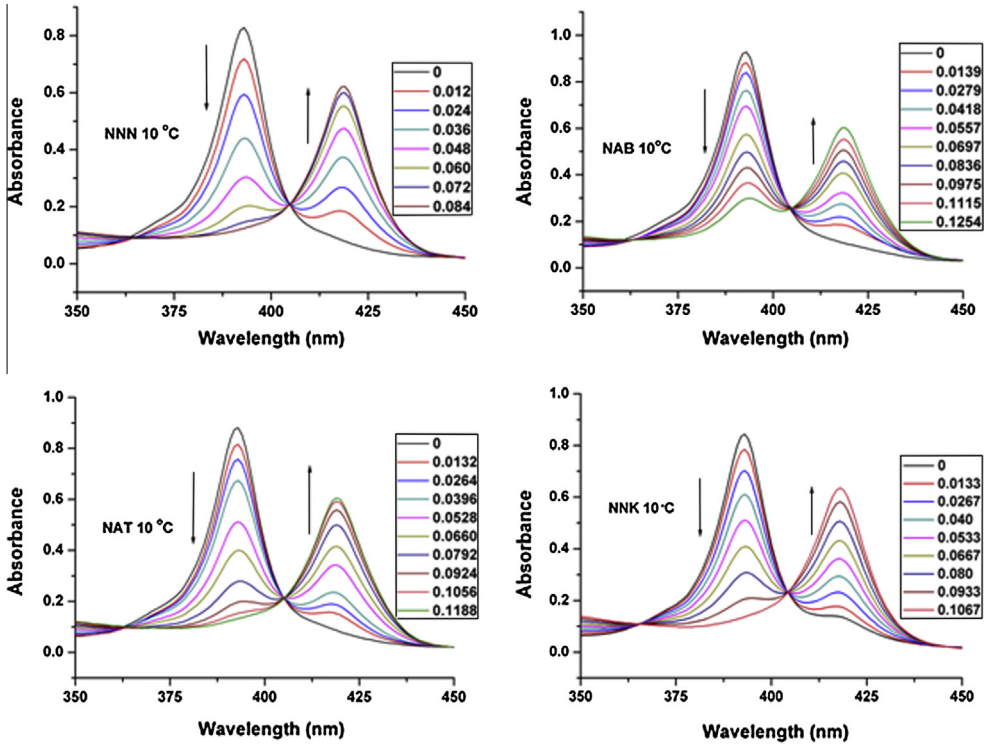

Fig. 3. Evolution of the UV–Vis spectra with various amounts of **TSNAs** (mmol/L) at 10 °C.

2.3. The interaction of CY-B with TSNAs by UV–Vis spectrum

The interaction between metalloporphyrin (**CY-B**) and **TSNAs** was investigated by UV–Vis spectrophotometer (Hitachi PharmaSpec UV-1900). A stock solution of the guest TSNAs (NNK & NNN & NAB & NAT) and host metalloporphyrin **(CY-B)** were prepared in dichloromethane. The concentration of guest TSNAs (NNK & NNN & NAB & NAT) was respectively 2.00×10^{-3} mol/L, 3.61×10^{-3} mol/L, 2.09×10^{-3} mol/L, 2.64×10^{-3} mol/L. The concentration of host metallporphyrin **CY-B** was 3.21×10^{-6} mol/L. Various amounts of TSNAs (NNK & NNN & NAB & NAT) were added to the solution of host metalloporphyrin (**CY-B**, 3 mL) then the spectrum were recorded to obtain the metalloporphyrin UV–Vis spectrum.

2.4. Benesi–Hildebrand UV–Vis liner fit plot of *CY-B* with TSNAs

The change in absorption of the metalloporphyrin (**CY-B**) following the addition of **TSNAs** conformed to the Benesi–Hildebrand equation [15] (Eq. (1)).

$$\frac{1}{A - A_0} = \frac{1}{K(A_{max} - A_0)[\text{TSNAs}]^2} + \frac{1}{A_{max} - A_0} \quad (1)$$

in which A_0 is the absorbance of metallporphyrin **CY-B**, A is the absorbance obtained with **TSNAs**, A_{max} is the absorbance obtained with excess amount of **TSNAs**, K is the association constant, and [TSNAs] is the concentration of TSNAs added. The binding constant K and the interaction between the metallporphyrin (**CY-B**) and

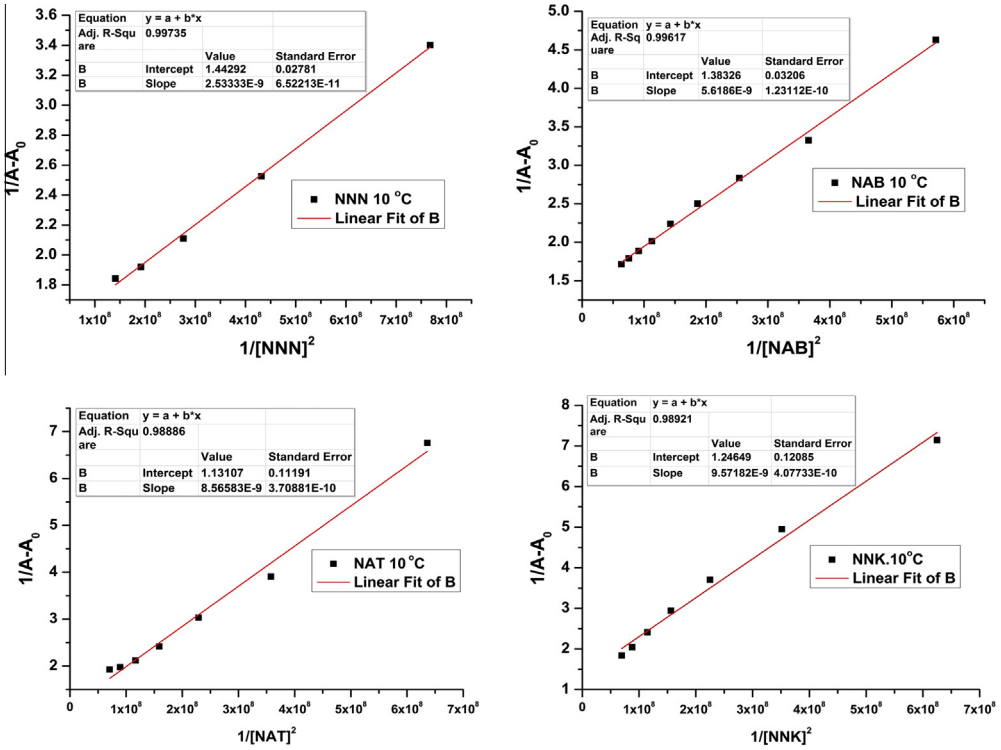

Fig. 4. B–H UV–Vis plot of **CY-B** with **TSNAs** at 10 °C.

Table 1
The association constant of host–guest coordination reaction in different temperature (CH_2Cl_2).

	Guest	Association constant (K, M^{-2})			
		5 °C	10 °C	15 °C	20 °C
Host (CY-B)	NNN	7.83×10^8 (0.995)	5.70×10^8 (0.997)	4.19×10^8 (0.997)	3.26×10^8 (0.991)
	NAB	3.10×10^8 (0.998)	2.46×10^8 (0.996)	1.95×10^8 (0.999)	1.32×10^8 (0.996)
Host (CY-B)	NNN	7.83×10^8 (0.995)	5.70×10^8 (0.997)	4.19×10^8 (0.997)	3.26×10^8 (0.991)
	NAB	3.10×10^8 (0.998)	2.46×10^8 (0.996)	1.95×10^8 (0.999)	1.32×10^8 (0.996)
	NAT	2.07×10^8 (0.994)	1.32×10^8 (0.989)	1.13×10^8 (0.996)	8.67×10^7 (0.999)
	NNK	1.79×10^8 (0.982)	1.30×10^8 (0.989)	1.09×10^8 (0.995)	7.79×10^7 (0.998)

Note: () indicate liner correlation coefficients.

TSNAs are positively correlated. Larger binding constants indicate stronger interaction between the metallporphyrin **CY-B** and TSNAs.

2.5. The HR-MS measure of complex

The interaction complex of **CY-B** with **TSNAs** was also investigated by high-resolution mass spectrometry after the addition of TSNAs to metallporphyrin **(CY-B)**. When the characteristic absorption peak (at 393 nm) disappeared as the addition of **TSNAs** increased in UV–Vis spectrum and the last mixture was measured by HR-MS.

*2.6. The calculation of thermodynamic parameters of the reaction of CY-B with **TSNAs***

According to the Van't Hoff equation (Eq. (2)), a plot of $\ln K$ against $1/T$ will give a straight line. The change of enthalpy ($\Delta_r H_m^\theta$) and entropy ($\Delta_r S_m^\theta$) were determined from the slope and intercept of the liner equation. The change of Gibbs free energy ($\Delta_r G_m^\theta$) were obtained from Gibbs free energy formula (Eq. (3)).

$$\ln K^\theta = -\frac{\Delta_r H_m^\theta}{RT} + \frac{\Delta_r S_m^\theta}{R} \quad (2)$$

$$\Delta_r G_m^\theta = \Delta_r H_m^\theta - T\Delta_r S_m^\theta \quad (3)$$

3. Results and discussion

*3.1. Synthesis of metalloporphyrin **CY-B***

The cobalt porphyrin **CY-B** was easily prepared using cheap and abundant hemin as the starting material. The deferrous reaction of the porphyrin center and HBr addition to the double bond located outside porphyrin cycle were performed in a "one pot reaction" (Scheme 1). Importantly, the bromo-substituted compounds need not be purified and could be directly used in the subsequent step. The nucleophilic substitution of the Br group by the OMe group is associated with the esterification of carboxylic acid. Only simple procedures, such as basification, filtration and recrystallization, were needed to obtain the key intermediate (**CY-A**) followed by the metallization of **CY-A** to afford the titled **CY-B**.

3.2. Interaction of CY-B with TSNAs

First, the UV–Vis spectra of **CY-B** in the absence and presence of various **TSNAs** (NNK & NNN & NAB & NAT) at different temperatures were investigated. As depicted in Figs. 3 and S1–S4, upon the addition of the **TSNAs**, the characteristic absorption peak of **CY-B** at 393 nm decreased gradually, and a new absorption peak at approximately 418 nm gradually increased in intensity. A red

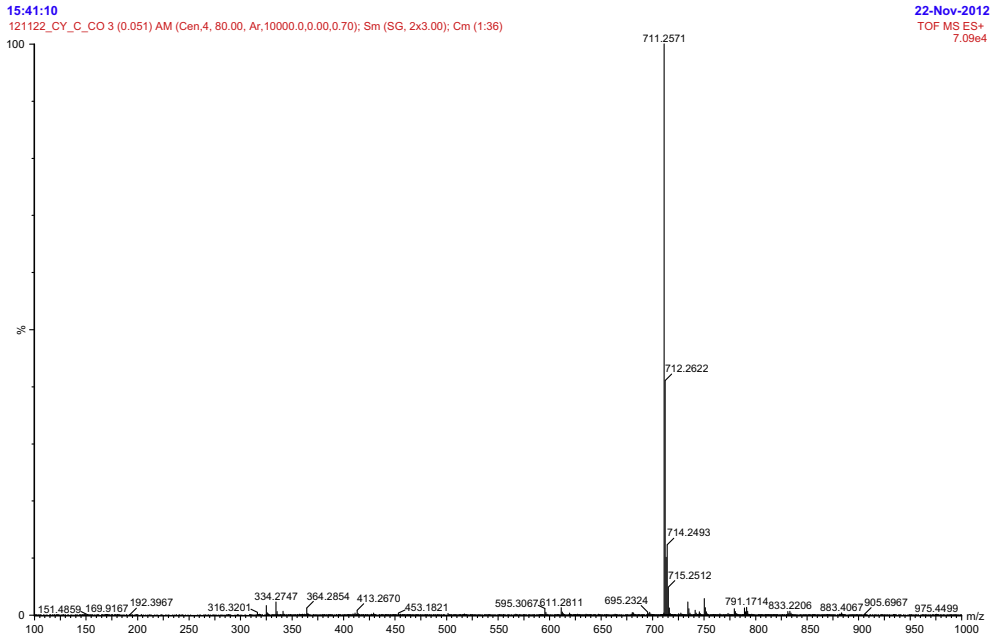

Fig. 5. HR-MS of **CY-B**.

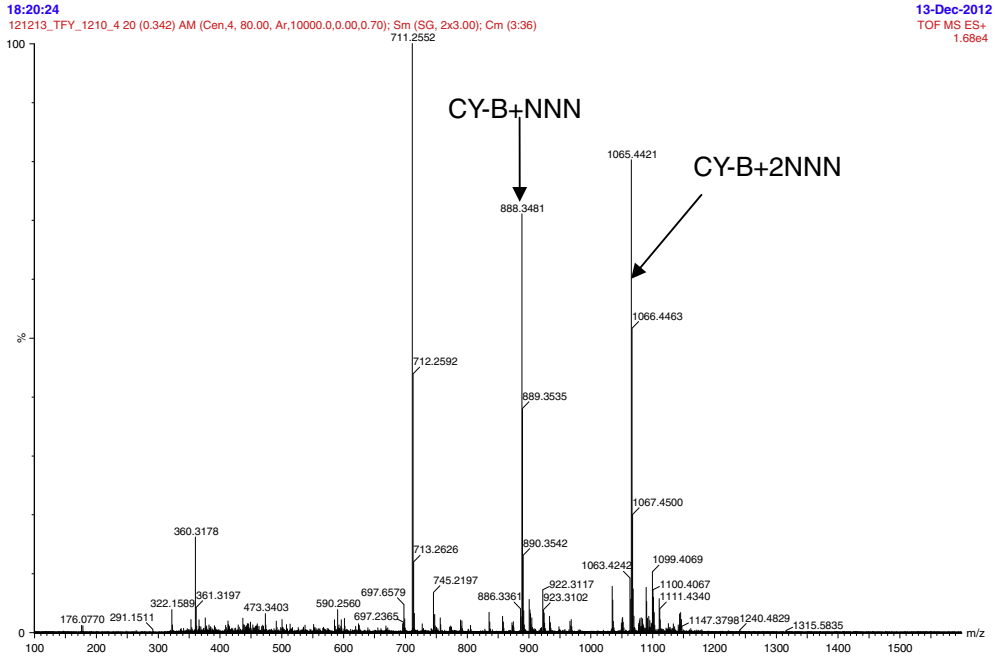

Fig. 6. HR-MS of **CY-B** with NNN.

shift (of approximately 20 nm) was observed in the UV–Vis spectrum, and an isosbestic point was identified. These results suggest that a new complex was formed when **CY-B** interacted with the **TSNAs**.

According to Eq. (1), the linear fit, coefficient, and association constant (K) were obtained from the $1/A - A_0$ and $1/[\text{TSNAs}]^2$ concentration curves (Figs. 4 and S5–S8). The plot of $1/(A - A_0)$ against $1/[\text{TSNAs}]^2$ exhibited a linear relationship, indicating that **CY-B** associates with **TSNAs** in a 1:2 stoichiometry. The association constants (K) between CY-B and the TSNAs was determined from the slope and intercept of the linear equation. The interaction association constants (K) ranged from $0.78 \times 10^8\ \text{M}^{-2}$ to $7.83 \times 10^8\ \text{M}^{-2}$, and the correlation coefficients (r) ranged from 0.982 to 0.999.

The high association constants (up to $10^8\ \text{M}^{-2}$) indicate that the interaction between the metalloporphyrin **CY-B** and the **TSNAs** was strong. The strength of the **CY-B** interaction with the TSNAs followed the trend: NNN > NAB > NAT > NNK (Table 1).

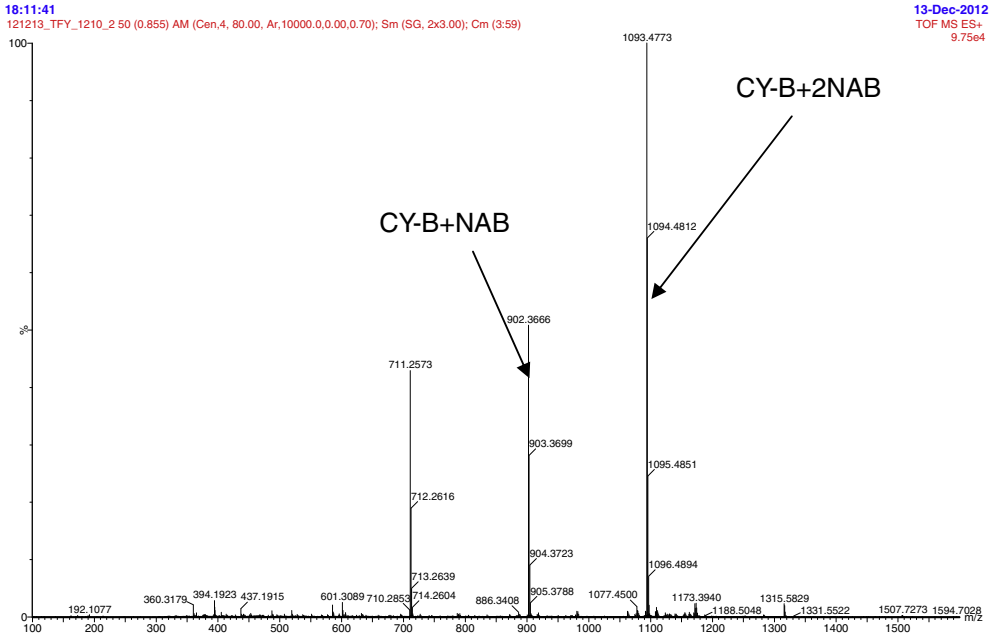

Fig. 7. HR-MS of **CY-B** with NAB.

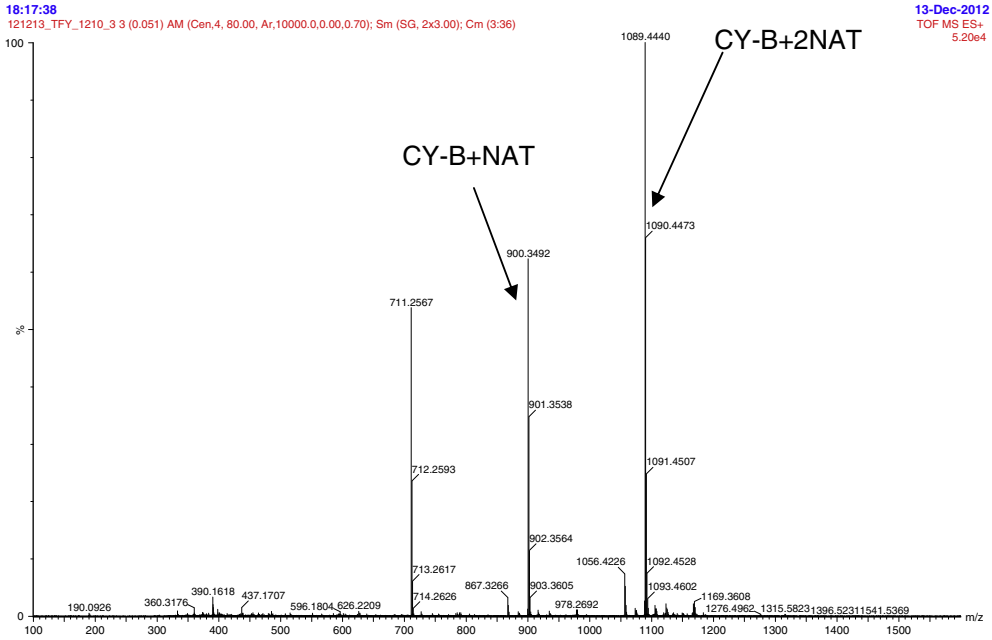

Fig. 8. HR-MS of **CY-B** with NAT.

The interaction of **CY-B** with the **TSNAs** was also investigated by high-resolution mass spectrometry. Following the addition of the TSNAs to **CY-B**, the mass spectra revealed that a complex of **CY-B** with two molecular TSNAs was formed, confirming that the host **CY-B** coordinated with two molecular guest TSNAs. Figs. 5–9 depict the mass spectrum of **CY-B** and of the complex of **CY-B** with the **TSNAs**.

According to the Van't Hoff equation (Eq. (2)), the plot of $\ln K$ against $1/T$ displays a linear relationship (Fig. 10). From the slope and intercept of the linear equation, the changes in enthalpy ($\Delta_r H_m^\theta$) and entropy ($\Delta_r S_m^\theta$) were calculated. According to the Gibbs free energy formula (Eq. (3)), the Gibbs free energy ($\Delta_r G_m^\theta$) values were obtained.

The thermodynamic parameters are outlined in Table 2. The results demonstrate that the reaction of the metalloporphyrin with the TSNAs was spontaneous and that the driving force for the reaction is a change in enthalpy. Increasing temperature inhibited the reaction.

A complex was also synthesized by the reaction of **CY-B** with NNN or NNK in dichloromethane. HR-MS of the complex indicate

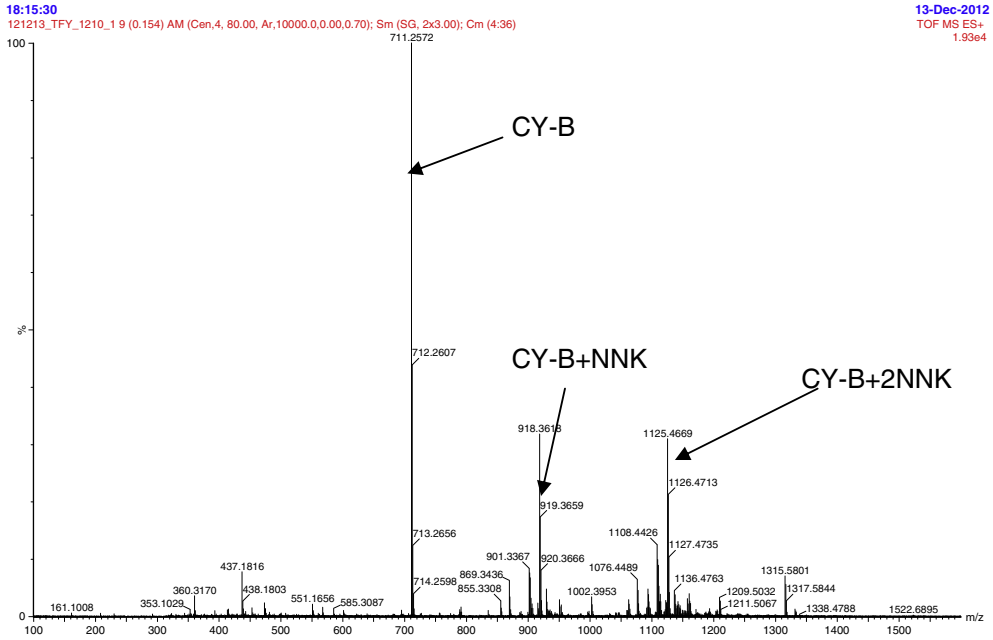

Fig. 9. HR-MS of **CY-B** with NNK.

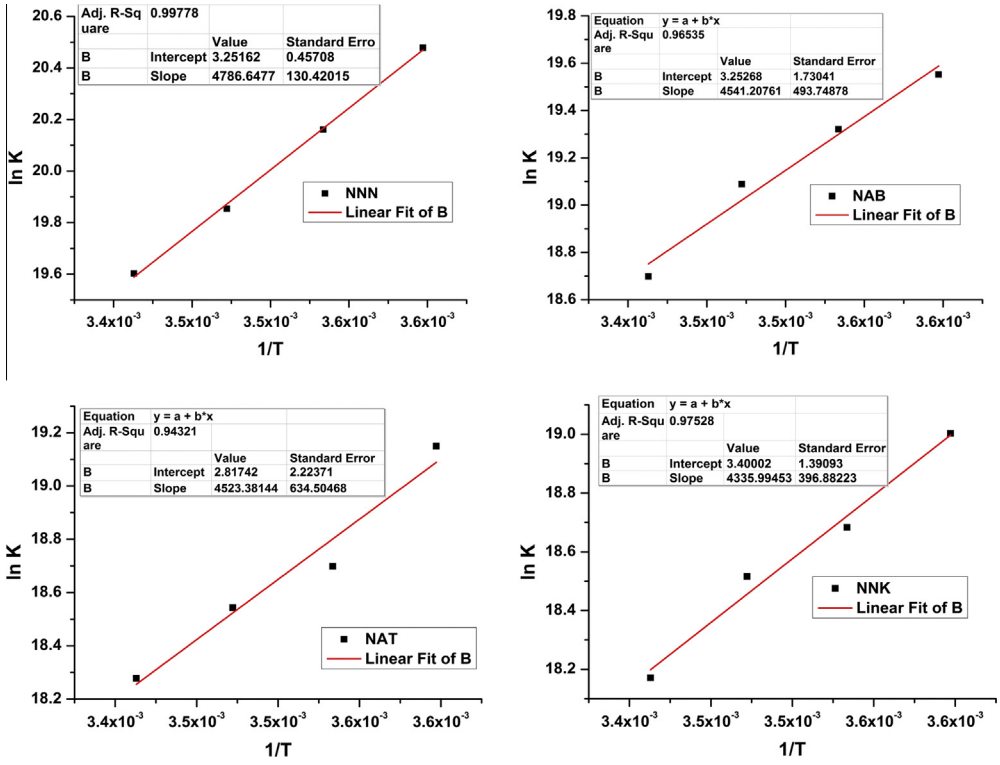

Fig. 10. Van't Hoff plot of ln$K$ against 1/T.

Table 2
The thermodynamic properties of reaction host **CY-B** with guest **TSNAs**.

Host	Guest	$-\Delta_r H_m^\theta$ (kJ mol^{-1})	$\Delta_r S_m^\theta$ (J K^{-1} mol^{-1})	$\Delta_r G_m^\theta$ (kJ mol^{-1})	r
CY-B	NNN	−40.15	27.28	−48.15	0.998
	NAB	−38.09	27.29	−46.22	0.965
	NAT	−37.94	23.63	−44.98	0.943
	NNK	−36.37	28.52	−44.87	0.975

Note: r is liner correlation coefficient.

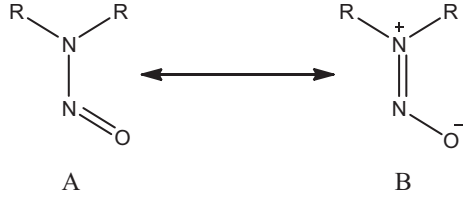

Fig. 11. Dipolar resonance contributions of nitrosamines.

CY-B coordinated with two molecular TSNAs. The IR spectra of the six-coordinate cobalt porphyrin complexes as KBr pellets exhibit peaks at 1282.9 cm^{-1} (CY-B-NNN) and 1239.3 cm^{-1} (CY-B-NNK) in the 1200–1300 cm^{-1} region, which can be attributed to the υ_{NO} and υ_{NN} for the coordinated nitrosamines (Figs. S9 and S10) [6]. This result suggests that the coordinated nitrosamines are best represented by a resonance hybrid with a significant contribution from structure B in Fig. 11.

4. Conclusion

In conclusion, a cobalt porphyrin **(CY-B)** was synthesized, and its interactions with **TSNAs** were studied. The results indicated that **TSNAs** can coordinate with **CY-B** in a ratio of 2:1; this stoichiometry is attributed to the ability of the —N—NO functional groups in the TSNAs to bond with the central Co of the porphyrin macrocycle. The thermodynamic properties of the interaction were also characterized. These results are important for the biological application of metalloporphyrins and further our understanding of the biological activity of metalloporphyrins *via* Type II interactions.

Acknowledgments

This project is supported by China Postdoctoral Science Foundation funded Project (2013M531963). This work was also financially supported by Chuanyu Branch of China Tobacco Corporation. We also thank the Analytical & Testing Center of Sichuan University for Sample Analysis.

Appendix A. Supplementary material

Supplementary data associated with this article can be found, in the online version, at http://dx.doi.org/10.1016/j.bioorg.2014.07.007.

References

[1] W. Lijinsky, Chemistry and Biology of N-Nitroso Compounds, Cambridge University Press, Cambridge, 1992.
[2] S.R. Tannenbaum, M.C. Archer, J.S. Wishnok, W.W. Bishop, J. Nat. Cancer Inst. 60 (1978) 251–253.
[3] (a) C.J. Michejda, M.B. Kroeger-koepke, S.R. Koepke, D.H. SiehNitrosamines, Activation of Nitrosamines to Biological Alkylating Agents, ACS Symposium Series, Springer, Berlin, 1981, pp. 3–20.;
(b) E. Okochi, M. Mochizuki, Chem. Pharm. Bull. 43 (1995) 2173–2176.
[4] (a) C.S. Yang, T.J. Smith, Adv. Exp. Med. Biol. 387 (1996) 385–394;
(b) S.S. Hecht, Chem. Res. Toxicol. 11 (1998) 559–603;
(c) G. Chowdhury, M.W. Calcutt, L.D. Nagy, F.P. Guengerich, Biochemistry 51 (2012) 9995–10007.
[5] K.E. Appel, H.H. Ruf, B. Mahr, M. Schwarz, R. Rickart, W. Kunz, Chem. Biol. Interact. 28 (1979) 17–33.
[6] N. Xu, L.E. Goodrich, N. Lehnert, D.R. Powell, G.B. Richter-Addo, Inorg. Chem. 49 (2010) 4405–4419.
[7] (a) Karl A. Wagner, Nancy H. Finkel, J. Eric Fossett, I. Gene Gillman, Anal. Chem. 77 (2005) 1001–1006;
(b) J.D. Adams, K.J. O'Mara-Adams, D. Hoffmann, Carcinogenesis 8 (1987) 729–731.
[8] K.D. Brunnemann, L. Genoble, D. Hoffmann, Carcinogenesis 8 (1987) 465–469.
[9] (a) P. Upadhyaya, S. Kalscheuer, J.B. Hochalter, P.W. Villalta, S.S. Hecht, Chem. Res. Toxicol. 21 (2008) 1468–1476;
(b) S. Zhang, M. Wang, P.W. Villalta, B.R. Lindgren, P. Upadhyaya, Y. Lao, S.S. Hecht, Chem. Res. Toxicol. 22 (2002) 926–936.
[10] (a) I. Stavridis, US5909736, 1999.;
(b) G. Deliconstantinos, V. Villiotou, J.C. Stavrides, Anticancer Res. 14 (1994) 2717–2726.
[11] C.G. Wang, Y. Dai, G.L. Feng, R. He, W.M. Yang, D.L. Li, X.Z. Zhou, L.J. Zhu, L.L. Tan, J. Agric. Food Chem. 59 (2011) 7172–7177.
[12] F.Y. Tao, C.G. Wang, K.Y. Ma, D.L. Li, L.L. Tan, J. Zhang, Y. Dai, X.Q. Yu, J. Porphyrins Phthalocyanines 17 (2013) 309–316.
[13] C.G. Wang, Y. Dai, S.M. Liu, W.M. Yang, Food Sci. 31 (2010) 109–113.
[14] J.E. Falk, Porphyrins and Metalloporphyrins, vol. 2, Elsevier, Amsterdam, 1964. p. 139.
[15] (a) H.A. Benesi, J.H. Hildebrand, J. Am. Chem. Soc. 71 (1949) 2703–2707;
(b) Y. Shiraishi, S. Sumiya, Y. Kohno, T. Hirai, J. Org. Chem. 73 (2008) 8571–8574;
c) M.I. Rodriguez-Caceres, R.A. Agbaria, I.M. Warner, J. Fluoresc. 15 (2005) 185–190.